

EFFECT OF TRANSVERSE SHEAR AND MATERIAL ORTHOTROPY IN A CRACKED SPHERICAL CAP

F. DELALE† and F. ERDOGAN

Lehigh University, Bethlehem, PA 18015, U.S.A.

(Received 10 May 1978; received for publication 5 July 1979)

Abstract—The elastostatic problem for a relatively thin-walled spherical cap containing a through crack is considered. The problem is formulated for a specially orthotropic material within the confines of a linearized, shallow shell theory. The theory used is equivalent to Reissner's theory of flat plates and hence permits the consideration of all five physical conditions on the shell boundaries separately. The solution of the problem is reduced to that of a pair of singular integral equations and the asymptotic stress state around the crack tips is investigated. The numerical solution of the problem is given for an isotropic shell and for two specially orthotropic shells. The results indicate that the material orthotropy as well as the shell curvature and thickness may have a considerable effect on the stress intensity factors at the crack tips.

1. INTRODUCTION

In structures consisting of relatively thin-walled curved sheets and containing a through crack the stress intensity factors calculated under the assumption of the cracked sheet being locally flat and that calculated from a bending theory of shells may differ quite considerably. This curvature effect has been amply demonstrated in a number of studies on a variety of shell and crack geometries (see, e.g. [1-4] for a crack in cylindrical shells and [3] in a spherical shell for typical results. Also, see [5] for typical asymptotic results in shells with a quadric surface and [6] for review and references). In these studies the so-called classical shallow shell theory is used to formulate the crack problem. The theory permits the use of only four conditions on the shell boundary. Hence, on the crack surface instead of prescribing twisting moment M_{ns} and transverse shear V_n separately, they are combined as the Kirchhoff effective transverse shear $V_n + \partial M_{ns}/\partial s$ and are given as a single boundary condition. The consequence of using such a first order theory which does not permit the satisfaction of all physical boundary conditions is well-known in the analogous plate bending problem. In using the classical plate bending theory and prescribing the normal component of the bending moment M_{nn} and the effective transverse shear $V_n + \partial M_{ns}/\partial s$ on the crack boundary, even though at the crack tips the bending moments appear to have the expected square-root singularity, the angular distribution of the bending stresses around the crack tips is found to be different from that of membrane stresses resulting from the in-plane loading of the plate and the results imply that the transverse shear V_n has a singularity of the order $r^{-3/2}$, r being the distance from the crack tip (see, e.g. [7]). On the other hand, as shown in [8-10], if a more refined theory such as that of Reissner [11] is used which permits the satisfaction of all physical conditions in M_{nn} , M_{ns} and V_n on the crack surface separately, it may be shown that the asymptotic behaviors of membrane and bending stress resultants around the crack tips are indeed identical and furthermore the transverse shear stress has no singularity.

The results found for the shells have been quite similar to that of flat plates. In limit when the curvature goes to zero the classical shell equations uncouple and give the two biharmonic equations for in-plane loading and bending of flat plates. Hence, as expected, the asymptotic results obtained from the classical shell theory show that the angular distributions of membrane and bending stress resultants are identical to those obtained for respectively the extension and the bending of flat plates. It is, therefore, apparent that as in the flat plate problem this inconsistency in the stress distribution near the crack surface arising from the use of the classical shell theory can be removed if a more refined shell theory is used to formulate the problem. Such a linearized shallow shell theory [12] is used in [13, 14] to solve the problems of a

†Permanent address: Technical University of Istanbul, Istanbul, Turkey.

cylindrical shell containing an axial and a circumferential crack, respectively. A similar theory is used in [15] to solve the problem of cracked spherical shell.† These solutions show that by using an appropriate shell theory which is consistent with the number of independent physical boundary conditions it is possible to obtain identical asymptotic distributions for bending and membrane stress resultants.

In this paper the problem of a shallow spherical cap containing a through crack is reconsidered. The problem is formulated by using the theory described in [12]. The solution is given for specially orthotropic as well as isotropic shells.

2. BASIC FORMULATION

Referring to Fig. 1, let N_{ij} , M_{ij} and V_i ($i, j = 1, 2$) be respectively membrane, moment, and transverse shear resultants in an arbitrary shallow shell. Under the assumptions generally associated with shallow shells the equilibrium equations may be expressed as‡[12]

$$N_{ij,j} = 0, \quad (2.1)$$

$$V_{i,i} + (Z_{,i}N_{ij})_{,j} + q(X_1, X_2) = 0, \quad (2.2)$$

$$M_{ij,j} - V_i = 0, \quad (i = 1, 2; \quad j = 1, 2) \quad (2.3)$$

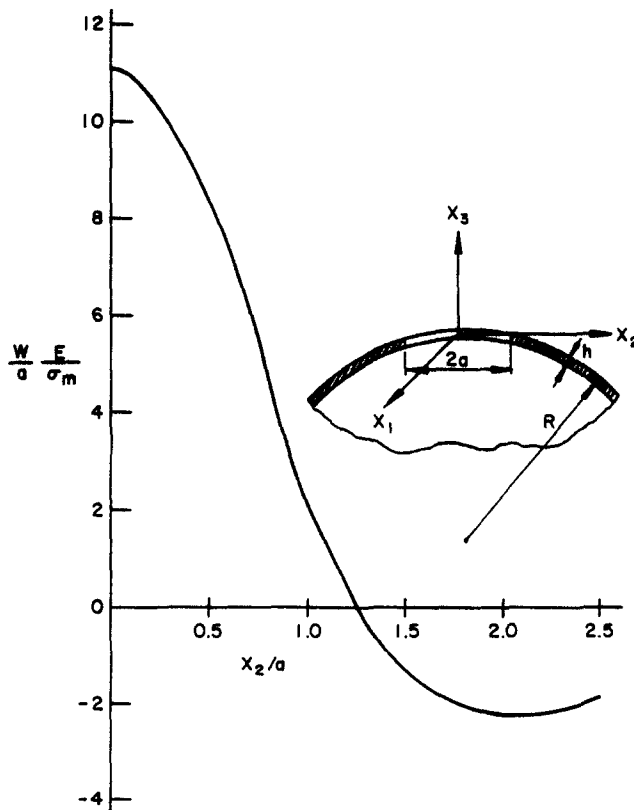


Fig. 1. The out-of-plane crack surface displacement in an isotropic spherical shell ($N_{11} \neq 0$, $M_{11} = 0$, $a/h = 5$, $\lambda_2 = 2$, $\nu = 1/3$).

†The difference between these two theories is that the terms u_i/R in the expressions of transverse shear strains and V_i/R in the membrane equilibrium equations are retained in [15] and are neglected in [13, 14]. However, since the results given in [15] and the isotropic shell results given in this paper are nearly identical, for the type of problems under consideration keeping these additional terms does not seem to be necessary.

‡In this section the summation convention and the indicial notation are used for conciseness.

where q is the surface loading and $Z(X_1, X_2)$ gives the perpendicular distance of the points on the middle surface of the shell to the tangent plane described by the rectangular axes X_1, X_2 . Let U_i, W and $\beta_i, (i = 1, 2)$ be respectively the X_i and the X_3 -components of the displacement and the angles of rotation of the normal to the shell surface. Since the constitutive equations relating the stress resultants N_{ij}, M_{ij} and V_i and the "displacement" quantities U_i, β_i and W involve first order differential operators, it is clear that expressed in terms of the five displacement quantities eqns (2.1)–(2.3) would give a system of five second order differential equations. Thus, prescribing a set of five boundary conditions in terms of U_i, β_i, W and their first derivatives the problem becomes a well-posed problem.

Let F be the stress function defined by

$$N_{ij} = e_{ik}e_{jl}F_{,kl}, \quad (i, j = 1, 2) \quad (2.4)$$

where e_{ik} is the permutation symbol.† Substituting from (2.4) it is seen that (2.1) is satisfied. Consider now the following stress-displacement relations

$$\epsilon_{ij} = a_{ijkl}N_{kl}/h = \frac{1}{2}[U_{i,j} + U_{j,i} + Z_{,i}W_{,j} + Z_{,j}W_{,i}], \quad (i, j = 1, 2) \quad (2.5)$$

where h is the shell thickness. Substituting from (2.4) and eliminating U_1 and U_2 , (2.5) becomes

$$e_{im}e_{jn}e_{kp}e_{lq}a_{ijkl}F_{,mnpq} + hZ_{,ij}e_{ik}e_{jl}W_{,kl} = 0. \quad (2.6)$$

A similar complicated differential equation is obtained from (2.2). For the general anisotropic material assumed in (2.5) even for very simple shell geometries these differential equations do not seem to be analytically tractable. However, as shown in [6], if one assumes the material to be specially orthotropic the related differential operators can be factorized and the problem becomes tractable. Writing the differential equations for an orthotropic material with constants E_1, ν_1, E_2, ν_2 and G_{12} , it can be shown that [6] the condition for factorization is

$$2G_{12} = \frac{\sqrt{(E_1E_2)}}{1 + \sqrt{(\nu_1\nu_2)}}. \quad (2.7)$$

The material satisfying (2.7) is said to be specially orthotropic. Defining

$$E = \sqrt{(E_1E_2)}, \quad \nu = \sqrt{(\nu_1\nu_2)}, \quad c = (E_1/E_2)^{1/4} \quad (2.8)$$

the relations between stress and displacement quantities in the shell may be expressed as

$$\epsilon_{11} = \frac{1}{hE}(N_{11}/c^2 - \nu N_{22}), \quad \epsilon_{12} = \frac{1+\nu}{hE}N_{12}, \quad \epsilon_{22} = \frac{1}{hE}(c^2N_{22} - \nu N_{11}), \quad (2.9)$$

$$M_{11} = D(c^2\beta_{1,1} + \nu\beta_{2,2}), \quad M_{12} = \frac{D(1-\nu)}{2}(\beta_{1,2} + \beta_{2,1}), \quad (2.10)$$

$$M_{22} = D(\nu\beta_{1,1} + \beta_{2,2}/c^2), \quad D = \frac{Eh^3}{12(1-\nu^2)},$$

$$\frac{V_1}{chB} = W_{,1} + \beta_1, \quad \frac{c}{hB}V_2 = W_{,2} + \beta_2, \quad B = \frac{5}{6} \frac{E}{2(1+\nu)} \quad (2.11)$$

where bending stresses are assumed to vary linearly in thickness direction and B is the effective shear modulus [11].

† $e_{11} = 0 = e_{22}, e_{12} = 1 = -e_{21}$.

Using the relations (2.9)–(2.11), the normalized quantities defined in Appendix A, and the curvatures defined by

$$\frac{\partial^2 Z}{\partial X_1^2} = -\frac{1}{R_1}, \quad \frac{\partial^2 Z}{\partial X_2^2} = -\frac{1}{R_2}, \quad \frac{\partial^2 Z}{\partial X_1 \partial X_2} = -\frac{1}{R_{12}}, \tag{2.12}$$

the differential eqns (2.6), (2.2) and (2.3) become

$$\nabla^4 \phi - \frac{1}{\lambda^2} \left(\lambda_1^2 \frac{\partial^2}{\partial y^2} - 2\lambda_{12}^2 \frac{\partial^2}{\partial x \partial y} + \lambda_2^2 \frac{\partial^2}{\partial x^2} \right) w = 0, \tag{2.13}$$

$$\nabla^4 w + \lambda^2 (1 - \kappa \nabla^2) \left(\lambda_1^2 \frac{\partial^2}{\partial y^2} - 2\lambda_{12}^2 \frac{\partial^2}{\partial x \partial y} + \lambda_2^2 \frac{\partial^2}{\partial x^2} \right) \phi = \lambda^4 (1 - \kappa \nabla^2) \frac{a}{h} q, \tag{2.14}$$

$$(1 - \kappa \nabla^2) \beta_x + \frac{\partial w}{\partial x} = \kappa \frac{1 + \nu}{2} \frac{\partial}{\partial y} \left(\frac{\partial \beta_y}{\partial x} - \frac{\partial \beta_x}{\partial y} \right), \tag{2.15}$$

$$(1 - \kappa \nabla^2) \beta_y + \frac{\partial w}{\partial y} = \kappa \frac{1 + \nu}{2} \frac{\partial}{\partial x} \left(\frac{\partial \beta_x}{\partial y} - \frac{\partial \beta_y}{\partial x} \right). \tag{2.16}$$

The normalizing constant a used in Appendix A is an additional length parameter in the shell which, in crack problems, is usually taken to be the half crack length. Defining the functions

$$\Omega(x, y) = \frac{\partial \beta_x}{\partial y} - \frac{\partial \beta_y}{\partial x}, \tag{2.17}$$

$$\psi(x, y) = \kappa \left(\frac{\partial \beta_x}{\partial x} + \frac{\partial \beta_y}{\partial y} \right) - w, \tag{2.18}$$

eqns (2.15)–(2.16) may be replaced by the following somewhat simpler equations[14]

$$\kappa \nabla^2 \psi - \psi - w = 0, \tag{2.19}$$

$$\frac{\kappa(1 - \nu)}{2} \nabla^2 \Omega - \Omega = 0. \tag{2.20}$$

3. SPHERICAL SHELL

Consider a specially orthotropic spherical shell which contains a meridional crack of length $2a$ along the X_2 axis. Thus, $\lambda_{12} = 0$ and, because of orthotropy, $\lambda_1 \neq \lambda_2$ (see Appendix A). Since we are interested in the stress perturbation problem in which crack surface tractions are the only external loads, without any loss in generality we may also assume that $q = 0$. Defining the operator

$$\nabla_\lambda^2 = \lambda_1^2 \frac{\partial^2}{\partial y^2} + \lambda_2^2 \frac{\partial^2}{\partial x^2}, \tag{3.1}$$

from (2.13) and (2.14) we obtain

$$\nabla^4 \nabla^4 \phi + \nabla_\lambda^2 \nabla_\lambda^2 (1 - \kappa \nabla^2) \phi = 0. \tag{3.2}$$

Let the solution of (3.2) be of the form

$$\phi(x, y) = \frac{1}{2\pi} \int_{-\infty}^{\infty} g(x, \alpha) e^{-i\alpha y} d\alpha. \tag{3.3}$$

From (3.2) and (3.3) it may be shown that the unknown function g vanishing at $x = \mp \infty$ may be expressed as

$$g(x, \alpha) = \begin{cases} \sum_1^4 R_j(\alpha) e^{m_j x}, & x > 0 \\ \sum_5^8 R_j(\alpha) e^{m_j x}, & x < 0 \end{cases} \quad (3.4)$$

where R_j , ($j = 1, \dots, 8$) are unknown and m_1, \dots, m_8 are the roots of the following characteristic equation

$$m^2 = p + \alpha^2, \\ p^4 - \kappa \lambda_2^4 p^3 + (2\kappa \lambda_1^2 \lambda_2^2 \alpha^2 - 2\kappa \lambda_2^4 \alpha^2 + \lambda_2^4) p^2 + (2\kappa \lambda_1^2 \lambda_2^2 \alpha^2 - \kappa \lambda_2^4 \alpha^2 - \kappa \lambda_1^4 \alpha^2 + 2\lambda_2^4 - 2\lambda_1^2 \lambda_2^2) \alpha^2 p + (\lambda_2^2 - \lambda_1^2)^2 \alpha^4 = 0 \quad (3.5)$$

satisfying

$$\text{Re}(m_j) < 0, \quad m_{j+4} = -m_j, \quad j = 1, \dots, 4. \quad (3.6)$$

Assuming the solution

$$w(x, y) = \frac{1}{2\pi} \int_{-\infty}^{\infty} f(x, \alpha) e^{-iy\alpha} d\alpha, \quad (3.7)$$

from (2.13) and (3.4) it may be shown that

$$f(x, \alpha) = \begin{cases} \lambda^2 \sum_1^4 \frac{R_j(\alpha) p_j^2}{\lambda_2^2 m_j^2 - \lambda_1^2 \alpha^2} e^{m_j x}, & x > 0, \\ \lambda^2 \sum_5^8 \frac{R_j(\alpha) p_j^2}{\lambda_2^2 m_j^2 - \lambda_1^2 \alpha^2} e^{m_j x}, & x < 0. \end{cases} \quad (3.8)$$

Similarly by assuming that

$$\Omega(x, y) = \frac{1}{2\pi} \int_{-\infty}^{\infty} h(x, \alpha) e^{-iy\alpha} d\alpha, \quad (3.9)$$

$$\psi(x, y) = \frac{1}{2\pi} \int_{-\infty}^{\infty} \theta(x, \alpha) e^{-iy\alpha} d\alpha, \quad (3.10)$$

from (2.20) and (2.19) it may be shown that

$$h(x, \alpha) = \begin{cases} A_1(\alpha) e^{r_1 x}, & x > 0, \\ A_2(\alpha) e^{r_2 x}, & x < 0, \end{cases} \quad (3.11)$$

$$\theta(x, \alpha) = \begin{cases} \lambda^2 \sum_1^4 \frac{R_j(\alpha) p_j^2}{(\kappa p_j - 1)(\lambda_2^2 m_j^2 - \lambda_1^2 \alpha^2)} e^{m_j x}, & x > 0 \\ \lambda^2 \sum_5^8 \frac{R_j(\alpha) p_j^2}{(\kappa p_j - 1)(\lambda_2^2 m_j^2 - \lambda_1^2 \alpha^2)} e^{m_j x}, & x < 0 \end{cases} \quad (3.12)$$

where

$$r_1 = -r_2 = -\left[\alpha^2 + \frac{2}{\kappa(1-\nu)} \right]^{1/2}. \quad (3.13)$$

The problem is thus reduced to the determination of unknown functions R_1, \dots, R_8, A_1 and A_2 which may be done by using the appropriate boundary conditions. In the spherical shell loaded symmetrically with respect to the plane of the crack (i.e. $x = 0$ plane) stress and moment resultants satisfy the following symmetry conditions:

$$\begin{aligned} N_{xx}(x, y) &= N_{xx}(-x, y), & N_{xy}(x, y) &= -N_{xy}(-x, y), \\ M_{xx}(x, y) &= M_{xx}(-x, y), & M_{xy}(x, y) &= -M_{xy}(-x, y), \\ V_x(x, y) &= -V_x(-x, y). \end{aligned} \tag{3.14}$$

Since (3.14) is valid for all x and y , in solving the problem it is sufficient to consider one half of the medium for which $x > 0$. Thus, there are only five unknowns R_1, \dots, R_4 and A_1 which may be determined by using five boundary conditions prescribed at $x = +0$.

Let the resultants N_{xy}, M_{xy} and V_x be zero on the crack surfaces. Then, because of assumed symmetry

$$N_{xy}(0, y) = 0, \quad M_{xy}(0, y) = 0, \quad V_x(0, y) = 0, \quad -\infty < y < \infty. \tag{3.15}$$

Equations (3.15) may be used to eliminate three of the five unknown functions R_1, \dots, R_4 and A_1 . The remaining two are determined by using the following mixed boundary conditions:

$$\lim_{x \rightarrow +0} N_{xx}(x, y) = F_1(y), \quad -\sqrt{c} < y < \sqrt{c}, \tag{3.16}$$

$$\lim_{x \rightarrow +0} M_{xx}(x, y) = F_2(y), \quad -\sqrt{c} < y < \sqrt{c}, \tag{3.17}$$

$$u(0, y) = 0, \quad \sqrt{c} < |y| < \infty, \tag{3.18}$$

$$\beta_x(0, y) = 0, \quad \sqrt{c} < |y| < \infty, \tag{3.19}$$

where F_1 and F_2 are known functions and $c = (E_1/E_2)^{1/4}$ (see Appendix A).

Using (3.3), (3.4) and (3.7)–(3.12), from the basic expressions given in the previous section the relevant components of the stress and moment resultants for $x > 0$ may be obtained as

$$N_{xx}(x, y) = -\frac{1}{2\pi} \int_{-\infty}^{\infty} \alpha^2 \sum_1^4 R_j(\alpha) e^{m_j x - i y \alpha} d\alpha, \tag{3.20}$$

$$N_{xy}(x, y) = -\frac{i}{2\pi} \int_{-\infty}^{\infty} \alpha \sum_1^4 m_j R_j(\alpha) e^{m_j x - i y \alpha} d\alpha, \tag{3.21}$$

$$\begin{aligned} M_{xx}(x, y) &= \frac{a}{h\lambda^4} \frac{1}{2\pi} \int_{-\infty}^{\infty} \lambda^2 \sum_1^4 \frac{R_j(\alpha) p_j^2 (m_j^2 - \nu \alpha^2)}{(\kappa p_j - 1)(\lambda_2^2 m_j^2 - \lambda_1^2 \alpha^2)} e^{m_j x - i y \alpha} d\alpha \\ &\quad - \frac{\kappa a (1 - \nu)^2}{2h\lambda^4} \frac{i}{2\pi} \int_{-\infty}^{\infty} \alpha r_1 A_1(\alpha) e^{r_1 x - i y \alpha} d\alpha, \end{aligned} \tag{3.22}$$

$$\begin{aligned} M_{xy}(x, y) &= -\frac{a(1 - \nu)}{h\lambda^4} \frac{i}{2\pi} \int_{-\infty}^{\infty} \lambda^2 \alpha \sum_1^4 \frac{R_j(\alpha) p_j^2 m_j}{(\kappa p_j - 1)(\lambda_2^2 m_j^2 - \lambda_1^2 \alpha^2)} e^{m_j x - i y \alpha} d\alpha \\ &\quad - \frac{\kappa a (1 - \nu)^2}{4h\lambda^4} \frac{1}{2\pi} \int_{-\infty}^{\infty} A_1(\alpha) (r_1^2 + \alpha^2) e^{r_1 x - i y \alpha} d\alpha, \end{aligned} \tag{3.23}$$

$$\begin{aligned} \frac{\partial V_x}{\partial y} &= -\kappa \lambda^2 \frac{i}{2\pi} \int_{-\infty}^{\infty} \alpha \sum_1^4 \frac{R_j(\alpha) p_j^3 m_j}{(\kappa p_j - 1)(\lambda_2^2 m_j^2 - \lambda_1^2 \alpha^2)} e^{m_j x - i y \alpha} d\alpha \\ &\quad - \frac{\kappa(1 - \nu)}{2} \frac{1}{2\pi} \int_{-\infty}^{\infty} \alpha^2 A_1(\alpha) e^{r_1 x - i y \alpha} d\alpha. \end{aligned} \tag{3.24}$$

Even though the mixed boundary conditions (3.16)–(3.19) would give a system of dual integral equations to determine the remaining two unknown functions, the problem may be reduced directly to a pair of integral equations by defining the following two new unknown functions:

$$\frac{\partial}{\partial y} u(+0, y) = G_1(y), \quad \frac{\partial}{\partial y} \beta_x(+0, y) = G_2(y). \quad (3.25)$$

Again, using the solution obtained in this section and the basic expressions given in the previous section, and observing that

$$\frac{\partial^2}{\partial y^2} u(+0, y) = -\frac{\partial^3}{\partial x^3} \phi(+0, y) + \frac{\lambda_2^2}{\lambda^2} \frac{\partial}{\partial x} w(+0, y),$$

it may be shown that

$$G_1(y) = -\frac{i}{2\pi} \int_{-\infty}^{\infty} \alpha^{-1} \sum_1^4 m_j^3 R_j(\alpha) e^{-i\alpha y} d\alpha \\ + \lambda_2^2 \frac{i}{2\pi} \int_{-\infty}^{\infty} \alpha^{-1} \sum_1^4 \frac{R_j(\alpha) p_j^2 m_j}{\lambda_2^2 m_j^2 - \lambda_1^2 \alpha^2} e^{-i\alpha y} d\alpha, \quad (3.26)$$

$$G_2(y) = -\lambda^2 \frac{i}{2\pi} \int_{-\infty}^{\infty} \alpha \sum_1^4 \frac{R_j(\alpha) p_j^2 m_j}{(\kappa p_j - 1)(\lambda_2^2 m_j^2 - \lambda_1^2 \alpha^2)} e^{-i\alpha y} d\alpha \\ - \frac{\kappa(1-\nu)}{2} \frac{1}{2\pi} \int_{-\infty}^{\infty} \alpha^2 A_1(\alpha) e^{-i\alpha y} d\alpha. \quad (3.27)$$

Thus, inverting (3.26), (3.27) and (3.21), (3.23) and (3.24) after substituting into (3.15), and using (3.18) and (3.19) the following system of algebraic equations is obtained:

$$A_1(\alpha) = 2f_2(\alpha), \quad (3.28)$$

$$\sum_1^4 m_j R_j(\alpha) = 0, \quad (3.29)$$

$$\sum_1^4 \frac{R_j(\alpha)(\lambda_2^2 p_j^2 m_j - \lambda_2^2 m_j^2 + \lambda_1^2 \alpha^2 m_j^3)}{\lambda_2^2 m_j^2 - \lambda_1^2 \alpha^2} = -i\alpha f_1(\alpha), \quad (3.30)$$

$$\sum_1^4 \frac{R_j(\alpha) p_j^2 m_j}{(\kappa p_j - 1)(\lambda_2^2 m_j^2 - \lambda_1^2 \alpha^2)} = \frac{i(1-\nu)\kappa}{2\alpha\lambda^2} (r_1^2 + \alpha^2) f_2(\alpha), \quad (3.31)$$

$$\sum_1^4 \frac{R_j(\alpha) p_j^3 m_j}{(\kappa p_j - 1)(\lambda_2^2 m_j^2 - \lambda_1^2 \alpha^2)} = \frac{i(1-\nu)}{\lambda^2} \alpha f_2(\alpha), \quad (3.32)$$

where

$$f_k(\alpha) = \int_{-\sqrt{c}}^{\sqrt{c}} G_k(t) e^{i\alpha t} dt, \quad (k = 1, 2). \quad (3.33)$$

Equations (3.29)–(3.32) may be solved giving R_1, \dots, R_4 in terms of f_1 and f_2 as follows:

$$R_j(\alpha) = i[Q_j(\alpha)f_1(\alpha) + N_j(\alpha)f_2(\alpha)], \quad j = 1, \dots, 4 \quad (3.34)$$

where Q_j and N_j , ($j = 1, \dots, 4$) are known functions.

4. THE INTEGRAL EQUATIONS

The analysis given in the previous section indicates that determination of the functions G_1 and G_2 would complete the solution of the problem. These functions are determined by using the boundary conditions (3.16) and (3.17). Thus, by substituting from (3.28), (3.33), (3.34), (3.20)

and (3.22) into (3.16) and (3.17) one obtains a system of integral equations of the following form:

$$\lim_{x \rightarrow +0} \int_{-\sqrt{c}}^{\sqrt{c}} \sum_1^2 G_j(t) dt \int_{-x}^{\infty} K_{kj}(\alpha, x) e^{-(t-y)\alpha} d\alpha = F_k(y), \quad k = 1, 2, \quad -\sqrt{c} < y < \sqrt{c}. \quad (4.1)$$

The functions $K_{kj}(\alpha, x)$ are bounded everywhere in $-\infty < \alpha < \infty$ and contain exponential damping terms of the form $\exp(m_j x)$, $\exp(r_j x)$, $\text{Re}(m_j) < 0$, $\text{Re}(r_j) < 0$. Since m_1, \dots, m_4 are not explicitly known functions of α , one needs to obtain asymptotic expressions for m_j as well as other terms in K_{kj} for large values of $|\alpha|$ in order to examine the singular behavior of the kernels in (4.1). Thus, from the characteristic equations (3.5) and (3.13) it can be shown that for large values of $|\alpha|$ we have

$$m_j(\alpha) = -|\alpha| \left(1 + \frac{p_j}{2\alpha^2} - \frac{p_j^2}{8\alpha^4} + \dots \right), \quad j = 1, \dots, 4, \quad (4.2)$$

$$r_1(\alpha) = -|\alpha| \left(1 + \frac{1}{\kappa(1-\nu)\alpha^2} - \dots \right) \quad (4.3)$$

where the roots $p_j(\alpha)$ are bounded for all values of α . The asymptotic values of K_{kj} ($k, j = 1, 2$) for large $|\alpha|$ may then be obtained by using (4.2) and (4.3). Adding and subtracting these values to and from K_{kj} in (4.1) one may easily separate the dominant part of the kernels. After carrying out this somewhat lengthy but straightforward analysis the integral equations and the kernels are found to be

$$\int_{-\sqrt{c}}^{\sqrt{c}} \frac{G_1(t)}{t-y} dt + \int_{-\sqrt{c}}^{\sqrt{c}} \sum_1^2 k_{1j}(y, t) G_j(t) dt = 2\pi F_1(y), \quad -\sqrt{c} < y < \sqrt{c}, \quad (4.4)$$

$$\frac{1-\nu^2}{\lambda^4} \int_{-\sqrt{c}}^{\sqrt{c}} \frac{G_2(t)}{t-y} dt + \int_{-\sqrt{c}}^{\sqrt{c}} \sum_1^2 k_{2j}(y, t) G_j(t) dt = 2\pi \frac{h}{a} F_2(y), \quad -\sqrt{c} < y < \sqrt{c}, \quad (4.5)$$

$$k_{11}(y, t) = \int_0^{\infty} \left[2 \sum_1^4 \alpha^2 Q_j(\alpha) - 1 \right] \sin \alpha(t-y) d\alpha, \quad (4.6)$$

$$k_{12}(y, t) = \int_0^{\infty} 2\alpha^2 \sum_1^4 N_j(\alpha) \sin \alpha(t-y) d\alpha, \quad (4.7)$$

$$k_{21}(y, t) = -\frac{2}{\lambda^2} \int_0^{\infty} \sum_1^4 \frac{p_j^2(m_j^2 - \nu\alpha^2) Q_j(\alpha)}{(\kappa p_j - 1)(\lambda^2 m_j^2 - \lambda_1^2 \alpha^2)} \sin \alpha(t-y) d\alpha, \quad (4.8)$$

$$k_{22}(y, t) = -\frac{2}{\lambda^4} \int_0^{\infty} \left[\lambda^2 \sum_1^4 \frac{p_j^2(m_j^2 - \nu\alpha^2) N_j(\alpha)}{(\kappa p_j - 1)(\lambda^2 m_j^2 - \lambda_1^2 \alpha^2)} - \kappa(1-\nu)^2 \alpha r_1 + (1-\nu^2)/2 \right] \sin \alpha(t-y) d\alpha \quad (4.9)$$

where the kernels $k_{ij}(y, t)$, ($i, j = 1, 2$) are bounded in the interval $-\sqrt{c} \leq (y, t) \leq \sqrt{c}$.

The index of the singular integral eqns (4.4) and (4.5) is +1. Consequently, the general solution of the system will contain two arbitrary constants [16]. The two additional conditions necessary to determine these constants are obtained from the boundary conditions (3.18) and (3.19) and the definition of G_1 and G_2 as given by (3.25). From these equations it follows that for u and β_x to be single-valued G_1 and G_2 must satisfy the following conditions:

$$\int_{-\sqrt{c}}^{\sqrt{c}} G_j(t) dt = 0, \quad (j = 1, 2). \quad (4.10)$$

For the convenience of solving the integral equations (4.4) and (4.5) numerically, following normalized quantities are defined:

$$\tau = t/\sqrt{c}, \quad \eta = y/\sqrt{c}, \quad \xi = x/\sqrt{c}, \quad H_1(\tau) = G_1(\sqrt{c}\tau), \quad H_2(\tau) = G_2(\sqrt{c}\tau). \quad (4.11)$$

The eqns (4.4), (4.5) and (4.10) would then become

$$\int_{-1}^1 \frac{H_1(\tau)}{\tau - \eta} d\tau + \sqrt{c} \int_{-1}^1 \sum_1^2 k_{ij}(\sqrt{c\eta}, \sqrt{c\tau}) H_j(\tau) d\tau = 2\pi F_1(\sqrt{c\eta}), \quad -1 < \eta < 1, \quad (4.12)$$

$$\frac{1 - \nu^2}{\lambda^4} \int_{-1}^1 \frac{H_2(\tau)}{\tau - \eta} d\tau + \sqrt{c} \int_{-1}^1 \sum_1^2 k_{2j}(\sqrt{c\eta}, \sqrt{c\tau}) H_j(\tau) d\tau = 2\pi \frac{h}{a} F_2(\sqrt{c\eta}), \quad -1 < \eta < 1, \quad (4.13)$$

$$\int_{-1}^1 H_j(\tau) d\tau = 0, \quad (j = 1, 2). \quad (4.14)$$

5. CRACK SURFACE DISPLACEMENTS

The analysis given in Sections 2 and 3 of this paper shows that once the unknown functions G_1 and G_2 are determined upon solving the integral eqns (4.4) and (4.5), all the field quantities in the shell may be obtained by evaluating certain integrals having G_1 and G_2 as density functions. One such group of quantities of practical interest is the stress and moment resultants on the plane of the crack, i.e. along $x = 0, |y| > \sqrt{c}$. Referring to (3.16) and (3.17) it may be noted that, aside from the factors 2π and $2\pi h/a$, (4.4) and (4.5) give the expressions for N_{xx} and M_{xx} for all values of y , i.e. for $-\infty < y < \infty, x = 0$. Thus, N_{xx} and M_{xx} for $|y| > \sqrt{c}$ may be evaluated from (4.4) and (4.5) by using the same kernels with $|y| > \sqrt{c}$ and the density functions $G_1(t)$ and $G_2(t), |t| < \sqrt{c}$.

Another group of quantities of physical interest is the crack surface displacements u and w , and the rotation β_x . From (3.18), (3.19) and (3.25) it may easily be seen that

$$u(+0, y) = - \int_y^{\sqrt{c}} G_1(t) dt, \quad -\sqrt{c} < y < \sqrt{c}, \quad (5.1)$$

$$\beta_x(+0, y) = - \int_y^{\sqrt{c}} G_2(t) dt, \quad -\sqrt{c} < y < \sqrt{c}. \quad (5.2)$$

The displacement component w which is perpendicular to the shell surface is given by (3.7) and may be expressed in terms of G_1 and G_2 by using the expressions (3.8), (3.34) and (3.33) as follows:

$$w(+0, y) = - \frac{\lambda^2}{\pi} \int_{-\sqrt{c}}^{\sqrt{c}} G_1(t) dt \int_0^\infty \sum_1^4 \frac{p_j^2 Q_j(\alpha)}{\lambda_2^2 m_j^2 - \lambda_1^2 \alpha^2} \sin \alpha(t - y) d\alpha - \frac{\lambda^2}{\pi} \int_{-\sqrt{c}}^{\sqrt{c}} G_2(t) dt \int_0^\infty \sum_1^4 \frac{p_j^2 N_j(\alpha)}{\lambda_2^2 m_j^2 - \lambda_1^2 \alpha^2} \sin \alpha(t - y) d\alpha, \quad (5.3)$$

where $Q_j(\alpha)$ and $N_j(\alpha), (j = 1, \dots, 4)$ are known functions.

6. ASYMPTOTIC FIELDS AROUND THE CRACK TIP

The index of the singular integral equations (4.12) and (4.13) is +1 and consequently the solution of the system is of the following form:

$$H_i(\eta) = h_i(\eta)(1 - \eta^2)^{-1/2}, \quad (i = 1, 2) \quad (6.1)$$

where h_1 and h_2 are bounded in $-1 \leq \eta \leq 1$. Using (6.1) and the relations [17, 6]

$$\int_0^\infty z^{\mu-1} e^{-sz} \left\{ \frac{\sin}{\cos} \right\} (rz) dz = \frac{\Gamma(\mu)}{(s^2 + r^2)^{\mu/2}} \left\{ \frac{\sin}{\cos} \right\} \left(\mu \tan^{-1} \frac{r}{s} \right), \quad (s > 0, \mu > 0), \quad (6.2)$$

$$\int_{-1}^1 \frac{h(\tau)}{\sqrt{(1-\tau^2)}} e^{i\beta\tau} d\tau = \left(\frac{\pi}{2|\beta|}\right)^{1/2} \left\{ h(1) \exp \left[i \left(\beta - \frac{\pi}{4} \frac{\beta}{|\beta|} \right) \right] + h(-1) \exp \left[-i \left(\beta - \frac{\pi}{4} \frac{\beta}{|\beta|} \right) \right] + o\left(\frac{1}{|\beta|}\right) \right\}, \quad (|\beta| \rightarrow \infty), \tag{6.3}$$

and going back to the original expressions such as (3.20)–(3.24) one could obtain asymptotic expressions for stress and moment resultants around the crack tip $\eta = 1, \xi = 0$. Following are typical such expressions:

$$N_{xx} \approx \frac{h_1(1)}{2\sqrt{(2\pi)}} \int_0^\infty \frac{1}{\sqrt{\beta}} (1 + |\xi|\beta) e^{-|\xi|\beta} \sin \left[(1-\eta)\beta - \frac{\pi}{4} \right] d\beta, \tag{6.4}$$

$$M_{xx} \approx \frac{h_2(1)}{2\sqrt{(2\pi)}} \frac{h}{12a} \int_0^\infty \frac{1}{\sqrt{\beta}} (1 + |\xi|\beta) e^{-|\xi|\beta} \sin \left[(1-\eta)\beta - \frac{\pi}{4} \right] d\beta, \tag{6.5}$$

$$V_x = \frac{\xi}{\sqrt{(2\pi)}} \left[\frac{\kappa}{2} h_1(1)(\lambda\lambda_2)^2 - h_2(1) \right] \int_0^\infty \beta^{-1/2} e^{-|\xi|\beta} \sin \left[(1-\eta)\beta - \frac{\pi}{4} \right] d\beta. \tag{6.6}$$

If we now define the polar coordinates r, θ in η, ξ plane by

$$\xi = r \sin \theta, \quad \eta - 1 = r \cos \theta, \tag{6.7}$$

and observe that the membrane and bending components of the stresses are given by (see Appendix A)

$$\sigma_{ij}^m = N_{ij}, \quad \sigma_{ij}^b = \frac{12az}{h} M_{ij}, \quad (i, j = x, y), \tag{6.8}$$

from (6.4), (6.5), and similar expressions for the combined stress state $\sigma_{ij} = \sigma_{ij}^m + \sigma_{ij}^b, (i, j = x, y)$ we obtain

$$\sigma_{xx} \approx -\frac{h_1(1) + zh_2(1)}{2\sqrt{(2r)}} \left[\frac{5}{4} \cos \frac{\theta}{2} - \frac{1}{4} \cos \frac{5\theta}{2} \right], \tag{6.9}$$

$$\sigma_{yy} \approx -\frac{h_1(1) + zh_2(1)}{2\sqrt{(2r)}} \left[\frac{3}{4} \cos \frac{\theta}{2} + \frac{1}{4} \cos \frac{5\theta}{2} \right], \tag{6.10}$$

$$\sigma_{xy} \approx -\frac{h_1(1) + zh_2(1)}{2\sqrt{(2r)}} \left[-\frac{1}{4} \sin \frac{\theta}{2} + \frac{1}{4} \sin \frac{5\theta}{2} \right]. \tag{6.11}$$

Evaluating the integral from (6.6) one could also show that

$$V_x \approx \left[-\frac{\kappa}{2} h_1(1)(\lambda\lambda_2)^2 + h_2(1) \right] \left(\frac{r}{2}\right)^{1/2} \sin \theta \cos \frac{\theta}{2}. \tag{6.12}$$

For the symmetric problem under consideration the stress intensity factor at the crack tip is defined by

$$k_1(X_3) = \lim_{X_2 \rightarrow a} \sqrt{(2(X_2 - a))} \sigma_{11}(0, X_2, X_3). \tag{6.13}$$

Referring to the definitions given in Appendix A from (6.13) and (6.9) it then follows that

$$k_1(X_3) = -\frac{cE\sqrt{a}}{2} \left[h_1(1) + \frac{X_3}{a} h_2(1) \right]. \tag{6.14}$$

7. THE ISOTROPIC SHELL

For an isotropic spherical shell $\lambda_{12} = 0$, $\lambda_1 = \lambda_2$ and with $q = 0$ eqns (2.13) and (2.14) become

$$\nabla^4 \phi - \frac{\lambda_2^2}{\lambda^2} \nabla^2 w = 0, \quad (7.1)$$

$$\nabla^4 w + (\lambda \lambda_2)^2 (1 - \kappa \nabla^2) \nabla^2 \phi = 0, \quad (7.2)$$

which, with (2.19) and (2.20) provide the differential equations to solve the problem. From (7.1) and (7.2) eliminating w we obtain

$$\nabla^6 \phi - \kappa \lambda_2^4 \nabla^4 \phi + \lambda_2^4 \nabla^2 \phi = 0. \quad (7.3)$$

replacing (3.2) of the orthotropic shell. Again defining the solution of (7.3) by (3.3), the characteristic eqn (3.5) becomes

$$p^3 - \kappa \lambda_2^4 p^2 + \lambda_2^4 p = 0, \quad (7.4)$$

with the roots

$$p_{1,2} = \frac{\kappa \lambda_2^4}{2} \left(1 \pm \sqrt{\left(1 - \frac{4}{\kappa^2 \lambda_2^4} \right)} \right), \quad p_3 = 0. \quad (7.5)$$

In this case having only two distinct roots which are known in closed form makes the analysis considerably simpler than that required for the orthotropic shell (and also for the isotropic cylindrical shell). Following the procedure outlined in Section 4 of this paper, one again obtains a system of singular integral equations identical to (4.4) and (4.5) with the difference that $c = 1$ and the kernels k_{ij} , ($i, j = 1, 2$) are now found to be

$$k_{11}(y, t) = \int_0^\infty \left[\frac{2\alpha^3}{K} \left(\frac{1}{m_1} - \frac{1}{m_2} \right) - 1 \right] \sin [(t - y)\alpha] \, d\alpha, \quad (7.6)$$

$$k_{12}(y, t) = \frac{1 - \nu}{\lambda^2 \lambda_2^2} \int_0^\infty \left[\frac{2\alpha^3}{K} \left(\frac{p_1}{m_1} - \frac{p_2}{m_2} \right) + \frac{\lambda_2^4}{K} \alpha \kappa (r_1^2 + \alpha^2) \left(\frac{1}{m_2} - \frac{1}{m_1} \right) + 2\alpha^2 \right] \times \sin [(t - y)\alpha] \, d\alpha, \quad (7.7)$$

$$k_{21}(y, t) = \frac{2}{\lambda^2 \lambda_2^2} \int_0^\infty \left[\frac{\alpha \lambda_2^4}{K} \left(\frac{m_2^2 - \nu \alpha^2}{p_2 m_2} - \frac{m_1^2 - \nu \alpha^2}{p_1 m_1} \right) + (1 - \nu) \alpha^2 \right] \sin [(t - y)\alpha] \, d\alpha, \quad (7.8)$$

$$k_{22}(y, t) = \frac{1}{\lambda^4} \int_0^\infty \left\{ -2\lambda_2^4 \frac{1 - \nu}{K} \left[\frac{m_1^2 - \nu \alpha^2}{p_1} \left(\frac{\alpha}{m_1 p_2} - \frac{\kappa (r_1^2 + \alpha^2)}{2\alpha m_1} \right) + \frac{m_2^2 - \nu \alpha^2}{p_2} \left(\frac{\kappa (r_1^2 + \alpha^2)}{2\alpha m_2} - \frac{\alpha}{m_2 p_1} \right) \right] + 2\kappa (1 - \nu)^2 \alpha r_1 - (1 - \nu^2) \right\} \sin [(t - y)\alpha] \, d\alpha, \quad (7.9)$$

$$K = \lambda_2^2 \sqrt{(\kappa^2 \lambda_2^4 - 4)}, \quad m_i^2 = p_i + \alpha^2, \quad (i = 1, 2),$$

$$r_1 = - \left[\alpha^2 + \frac{2}{\kappa(1 - \nu)} \right]^{1/2}. \quad (7.10)$$

8. THE RESULTS

The singular integral eqns (4.12)–(4.14) are solved by substituting from (6.1) and using the Gauss–Chebyshev integration formulas. Thus, (4.12)–(4.13) may be approximated by [18–20]

$$\sum_{j=1}^n W_j \left[\frac{h_1(\tau_j)}{\tau_j - \eta_i} + \sqrt{c} \sum_{m=1}^2 k_{1m}(\sqrt{c}\eta_i, \sqrt{c}\tau_j) h_m(\tau_j) \right] = 2\pi F_1(\sqrt{c}\eta_i), \quad (8.1)$$

$$i = 1, \dots, n - 1,$$

$$\sum_{j=1}^n W_j \left[\frac{1-\nu^2}{\lambda^4} \frac{h_2(\tau_j)}{\tau_j - \eta_i} + \sqrt{c} \sum_{m=1}^2 k_{2m}(\sqrt{c\eta_i}, \sqrt{c\tau_j}) h_m(\tau_j) \right] = 2\pi \frac{h}{a} F_2(\sqrt{c\eta_i}), \quad i = 1, \dots, n-1, \tag{8.2}$$

$$\sum_{j=1}^n W_j h_k(\tau_j) = 0, \quad k = 1, 2, \tag{8.3}$$

$$\tau_j = \cos \left(\pi \frac{j-1}{n-1} \right), \quad j = 1, \dots, n, \tag{8.4}$$

$$\eta_i = \cos \left(\pi \frac{2i-1}{2n-2} \right), \quad i = 1, \dots, n-1, \tag{8.5}$$

$$W_1 = W_n = \frac{\pi}{2(n-1)}, \quad W_j = \frac{\pi}{n-1}, \quad j = 2, \dots, n-1. \tag{8.6}$$

The numerical results are obtained for uniform and concentrated membrane and bending loads on the crack surfaces. Keeping in mind that superposition is permissible, the results for each load will be given separately. First we consider the uniform membrane loading, i.e.

$$N_{11}(0, X_2) = -N_{11} = -h\sigma_m, \quad M_{11}(0, X_2) = 0, \quad -a < X_2 < a, \tag{8.7}$$

or

$$F_1(\sqrt{c\eta}) = -\sigma_m/cE, \quad F_2(\sqrt{c\eta}) = 0, \quad -1 < \eta < 1. \tag{8.8}$$

Here the corresponding flat plate stress intensity factor is $\sigma_m \sqrt{a}$. Thus, from (6.14), it is seen that once $h_1(1)$ and $h_2(1)$ are obtained from the solution of the integral equations the membrane and bending stress intensity factor ratios may be calculated as

$$k_{mm} = \frac{k_1(0)}{\sigma_m \sqrt{a}} = -\frac{cE}{2\sigma_m} h_1(1), \tag{8.9}$$

$$k_{bm} = \frac{k_1(h/2) - k_1(0)}{\sigma_m \sqrt{a}} = -\frac{cE}{2\sigma_m} \frac{h}{2a} h_2(1). \tag{8.10}$$

The second loading condition considered is

$$N_{11}(0, X_2) = 0, \quad M_{11}(0, X_2) = -M_{11} = -\frac{h^2}{6} \sigma_b, \quad -a < X_2 < a, \tag{8.11}$$

or

$$F_1(\sqrt{c\eta}) = 0, \quad F_2(\sqrt{c\eta}) = -\frac{\sigma_b}{6cE}, \quad -1 < \eta < 1. \tag{8.12}$$

In this case, referring again to (6.14), the membrane and bending stress intensity factor ratios may be expressed as

$$k_{mb} = \frac{k_1(0)}{\sigma_b \sqrt{a}} = -\frac{cE}{2\sigma_b} h_1(1), \tag{8.13}$$

$$k_{bb} = \frac{k_1(h/2) - k_1(0)}{\sigma_b \sqrt{a}} = -\frac{cE}{2\sigma_b} \frac{h}{2a} h_2(1). \tag{8.14}$$

In the numerical analysis the effective transverse shear modulus is assumed to be $B = 5G/6$.

(a) *Isotropic shells*

For an isotropic spherical shell with a Poisson's ratio $\nu = 1/3$ the calculated results are shown in Tables 1-4. One may note that aside from the standard shell parameter λ_2 which appears in the classical shell theory, the results given in this paper depend on an additional parameter a/h which, within the confines of the shallow shell theory, gives the thickness effect.

Table 1. The stress intensity factor ratio k_{mm} for an isotropic spherical shell ($N_{11} \neq 0$, $M_{11} = 0$, $\nu = 1/3$)

λ_2	$a/h = 0.5$	$a/h = 1.0$	$a/h = 2$	$a/h = 5$	$a/h = 10$
0.00	1.000	1.000	1.000	1.000	1.000
0.25	1.021	1.019	1.019	1.018	1.018
0.50	1.094	1.076	1.071	1.069	1.069
0.75		1.173	1.156	1.150	1.149
1.00		1.305	1.268	1.255	1.252
1.5			1.556	1.519	1.512
2.0			1.918	1.841	1.828
2.5				2.208	2.186
3.0				2.615	2.579
3.5				3.058	3.004
4.0				3.539	3.460

Table 2. The stress intensity factor ratio k_{hh} for an isotropic spherical shell ($N_{11} \neq 0$, $M_{11} = 0$, $\nu = 1/3$)

λ_2	$a/h = 0.5$	$a/h = 1$	$a/h = 2$	$a/h = 5$	$a/h = 10$
0.00	0.000	0.000	0.000	0.000	0.000
0.25	0.041	0.037	0.035	0.034	0.033
0.50	0.095	0.090	0.086	0.084	0.084
0.75		0.133	0.130	0.130	0.130
1.0		0.157	0.158	0.162	0.165
1.5			0.155	0.174	0.187
2.0			0.077	0.117	0.142
2.5				-0.010	0.031
3.0				-0.206	-0.146
3.5				-0.471	-0.390
4.0				-0.807	-0.701

Table 3. The stress intensity factor ratio k_{hh} for an isotropic spherical shell ($N_{11} = 0$, $M_{11} \neq 0$, $\nu = 1/3$)

λ_2	$a/h = 0.5$	$a/h = 1$	$a/h = 2$	$a/h = 5$	$a/h = 10$
0.00		0.752	0.704	0.667	0.652
0.25	0.808	0.740	0.694	0.659	0.645
0.50	0.772	0.709	0.669	0.638	0.626
0.75		0.670	0.635	0.609	0.599
1.0		0.630	0.598	0.577	0.569
1.5			0.526	0.511	0.506
2.0			0.465	0.451	0.448
2.5				0.401	0.399
3.0				0.360	0.359
3.5				0.327	0.325
4.0				0.300	0.297

Table 4. The stress intensity factor ratio k_{mb} for an isotropic spherical shell ($N_{11} = 0$, $M_{11} \neq 0$, $\nu = 1/3$)

λ_2	$a/h = 0.5$	$a/h = 1$	$a/h = 2$	$a/h = 5$	$a/h = 10$
0.00	0.000	0.000	0.000	0.000	0.000
0.25	0.013	0.011	0.010	0.008	0.008
0.50	0.032	0.028	0.024	0.021	0.020
0.75		0.044	0.039	0.034	0.032
1.0		0.058	0.052	0.046	0.043
1.5			0.071	0.064	0.061
2.0			0.083	0.076	0.073
2.5				0.084	0.081
3.0				0.089	0.086
3.5				0.092	0.089
4.0				0.094	0.091

The values given for $\lambda_2 = 0$ correspond to and agree with the flat plate results[9, 10]. For $a/h = 10$ calculated values of k_{mm} are indistinguishable from the classical shell theory results[3]. However, the remaining stress intensity ratios are quite different. Also the results found in this paper for the isotropic shell are nearly identical to those found in [15] indicating that the effect of the additional terms u_i/R and V_i/R retained in [15] in the expressions of transverse shear strains and membrane equilibrium equations, respectively, on the stress intensity factors are not significant.

Examples for the crack surface displacement w perpendicular to the shell surface for a uniform membrane loading $N_{11} = h\sigma_m$ or a bending moment $M_{11} = h^2\sigma_b/6$ are shown in Figs. 1 and 2, respectively. Even though around the crack the shell bulges out, as observed in cylindrical shells[6, 14], some distance ahead of the crack tip w becomes negative.

Concentrated membrane forces and moments on the crack surfaces are used as a third kind of loading in the isotropic shell. If the shell is under symmetrically applied concentrated membrane forces on the crack surfaces given by†

$$N_{11}(0, X_2) = -N_0[\delta(X_2 - ay_i) + (X_2 + ay_i)], \quad (8.15)$$

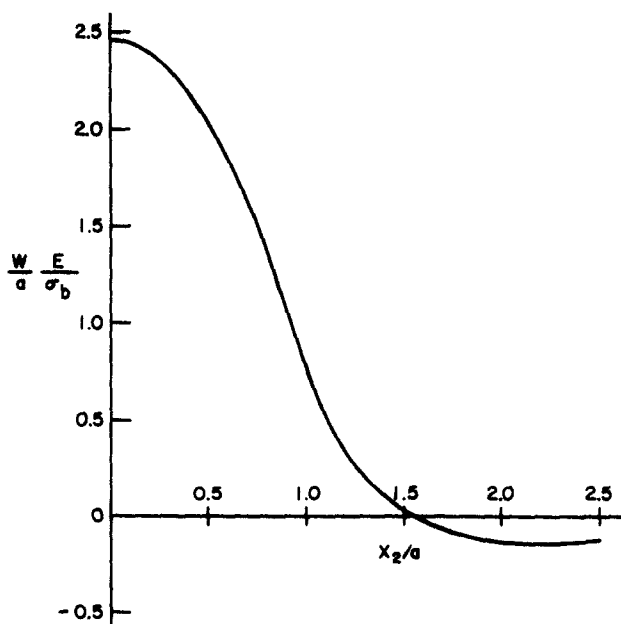


Fig. 2. The out-of-plane crack surface displacement in an isotropic spherical shell ($N_{11} = 0$, $M_{11} \neq 0$, $a/h = 5$, $\lambda_2 = 2$, $\nu = 1/3$).

†In the type of numerical procedure used in this paper (indeed, generally speaking, in any type of numerical procedure) it is not possible to handle ideally concentrated input functions such as those given by (8.15) and (8.17). In calculating the results given in Table 5 the concentrated loads are approximated by triangular distributions having an area of N_0 or M_0 .

the stress intensity factor ratios may be defined as

$$k_{mm} = \frac{k_1(0)}{(N_0/ha)\sqrt{a}}, \quad k_{bm} = \frac{k_1(h/2) - k_1(0)}{(N_0/ha)\sqrt{a}}. \quad (8.16)$$

Similarly, for concentrated moments

$$M_{11}(0, X_2) = -M_0[\delta(X_2 - ay_i) + \delta(X_2 + ay_i)]. \quad (8.17)$$

The stress intensity ratios may be expressed as

$$k_{mb} = \frac{k_1(0)}{(6M_0/ah^2)\sqrt{a}}, \quad k_{bb} = \frac{k_1(h/2) - k_1(0)}{(6M_0/ah^2)\sqrt{a}}. \quad (8.18)$$

Table 5 shows the results of an example giving the stress intensity factors defined by (8.16) and (8.18). Note that at $y = 0$ the concentrated loads are $2N_0$ and $2M_0$.

Using the numerical procedure outlined in this section one could also obtain the "Green's functions" for the stress intensity factors. These results may be useful in solving the shell problems in which the crack surface tractions for the perturbation problem are not uniform. For example, if the crack surface tractions are

$$N_{11}(0, X_2) = N_{11}(0, -X_2) = -N(ay) \quad (8.19)$$

$$M_{11}(0, X_2) = M_{11}(0, -X_2) = -M(ay) \quad (8.20)$$

then the membrane and bending components of the stress intensity factors may be expressed as

$$k_1(0) = \sum_{i=1}^{n/2} \left[G_{mm}(y_i) \frac{N(ay_i)}{h} \sqrt{a} + G_{mb}(y_i) \frac{6M(ay_i)}{h^2} \sqrt{a} \right], \quad (8.21)$$

$$k_1(h/2) - k_1(0) = \sum_{i=1}^{n/2} \left[G_{bm}(y_i) \frac{N(ay_i)}{h} \sqrt{a} + G_{bb}(y_i) \frac{6M(ay_i)}{h^2} \sqrt{a} \right]. \quad (8.22)$$

For one specific shell geometry namely, for $a/h = 5$ and $\lambda_2 = 3$ the Green's functions G_{jk} , ($j, k = m, b$) are given by Table 6. Needless to say, the numerical procedure for evaluating G_{jk} is extremely simple and basically amounts to the repeated solution of the system of linear algebraic equations by taking only one row of the input columns $F_1(y_i)$ and $F_2(y_i)$ to be nonzero at each run.

(b) Specially orthotropic shells

To give an example for specially orthotropic shells we consider two real materials namely, titanium which is a mildly orthotropic material and graphite which is severely orthotropic. The elastic properties of these materials and the average shear modulus calculated from (2.7), that is

$$G_{ave} = \frac{\sqrt{(E_1 E_2)}}{2(1 + \sqrt{(\nu_1 \nu_2)})} \quad (8.23)$$

Table 5. Stress intensity factor ratios for an isotropic spherical shell under concentrated forces ($a/h = 5$, $\lambda_2 = 3$, $\nu = 1/3$)

y_i	k_{mm}	k_{bm}	k_{bb}	k_{mb}
0.89	2.251	0.096	0.794	0.052
0.74	2.205	-0.006	0.299	0.075
0.53	2.499	-0.201	0.132	0.095
0.28	2.785	-0.389	0.044	0.110
0.00	2.900	-0.466	0.016	0.116

Table 6. Green's functions for membrane and bending stress intensity factors in symmetrically loaded isotropic spherical shell ($a/h = 5$, $\lambda_2 = 3$, $\nu = 1/3$)

y_i	$G_{mm}(y_i)$	$G_{bm}(y_i)$	$G_{bd}(y_i)$	$G_{mb}(y_i)$
0.98982	0.19074	0.00216	0.16655	0.00075
0.90963	0.26344	0.01125	0.09298	0.00608
0.75575	0.40686	-0.00110	0.05519	0.01386
0.54064	0.59218	-0.04768	0.03140	0.02245
0.28173	0.75294	-0.10516	0.01202	0.02967
0.0	0.40856	-0.06573	0.00226	0.01622

Table 7. Elastic constants of the materials used in the examples (see insert in Fig. 3)

	Titanium	Graphite
E_1 (psi)	15.07×10^6	1.5×10^6
E_2 (psi)	20.8×10^6	40×10^6
ν_1	0.1966	0.0075
ν_2	0.2714	0.2000
G_{12} (psi)	6.78×10^6	4.0×10^6
G_{ave} (psi)	7.15×10^6	3.73×10^6

Table 8. The stress intensity factor ratio k_{mm} for a titanium spherical shell ($N_{11} \neq 0$, $M_{11} = 0$, $\lambda_0^4 = 12(1 - \nu^2)a^4/h^2R^2$, $\nu = \sqrt{(\nu_1\nu_2)}$)

λ_0	$a/h = 10$		$a/h = 5$		$a/h = 2$		$a/h = 1$	
	$E_1/E_2 = 0.725$	$E_1/E_2 = 1.380$	$E_1/E_2 = 0.725$	$E_1/E_2 = 1.380$	$E_1/E_2 = 0.725$	$E_1/E_2 = 1.380$	$E_1/E_2 = 0.725$	$E_1/E_2 = 1.380$
0.0	1.000	1.000	1.000	1.000	1.000	1.000	1.000	1.000
0.25	1.016	1.021	1.016	1.021	1.016	1.021	1.017	1.022
0.50	1.060	1.077	1.060	1.077	1.062	1.079	1.065	1.084
0.75	1.129	1.164	1.130	1.165	1.135	1.171	1.148	1.187
1.0	1.220	1.276	1.222	1.279	1.232	1.291	1.262	1.327
1.5	1.450	1.555	1.456	1.561	1.486	1.596		
2.0	1.733	1.891	1.744	1.903	1.807	1.976		
2.5	2.056	2.270	2.076	2.291				
3.0	2.415	2.685	2.446	2.718				
3.5	2.806	3.132	2.852	3.183				
4.0	3.226	3.611	3.296	3.687				

are shown in Table 7. It may be seen that in both materials the measured shear modulus G_{12} is sufficiently close to the calculated value G_{ave} to warrant the assumption of special orthotropy.

Tables 8–15 show the stress intensity factor ratios defined by (8.9) and (8.10) for a shell under uniform membrane loading and by (8.13) and (8.14) for a shell under uniform bending. Note that in each case the tables give the results for a crack parallel and for that perpendicular to the stiffer axis of orthotropy (see Table 7 and the insert in Fig. 3). The results have been tabulated by using a/h and a parameter λ_0 defined by

$$\lambda_0 = [12(1 - \nu_1\nu_2)]^{1/4} a/\sqrt{Rh} \tag{8.24}$$

as the variables. The choice of λ_0 stems from the fact that the shell parameters λ_1 and λ_2 are dependent on the orientation of the crack relative to the axes of orthotropy. In order to show the comparison between the isotropic results and those obtained from an orthotropic shell with two different crack orientations some of the results are displayed graphically in Figs. 3 and 4. The figures show that the isotropic results are bracketed by the two sets of results obtained for the orthotropic shell with the crack parallel and perpendicular to the stiffer axis of orthotropy. It is also seen that the material orthotropy may have a very significant effect on the stress intensity factors.

Table 9. The stress intensity factor ratio k_{ab} for a titanium spherical shell ($N_{11} \neq 0, M_{11} = 0$)

λ_0	a/h = 10		a/h = 5		a/h = 2		a/h = 1	
	$E_1/E_2 =$	$E_1/E_2 =$	$E_1/E_2 =$	$E_1/E_2 =$	$E_1/E_2 =$	$E_1/E_2 =$	$E_1/E_2 =$	$E_1/E_2 =$
	0.725	1.380	0.725	1.380	0.725	1.380	0.725	1.380
0.0	0.000	0.000	0.000	0.000	0.000	0.000	0.000	0.000
0.25	0.025	0.029	0.026	0.030	0.027	0.031	0.029	0.033
0.50	0.065	0.073	0.066	0.074	0.068	0.075	0.071	0.079
0.75	0.104	0.115	0.104	0.115	0.106	0.115	0.109	0.118
1.0	0.135	0.148	0.134	0.145	0.133	0.142	0.134	0.141
1.5	0.165	0.175	0.158	0.164	0.145	0.146		
2.0	0.146	0.145	0.129	0.121	0.099	0.083		
2.5	0.077	0.054	0.047	0.015				
3.0	-0.044	-0.099	-0.090	-0.158				
3.5	-0.219	-0.317	-0.283	-0.398				
4.0	-0.448	-0.602	-0.533	-0.709				

Table 10. The stress intensity factor ratio k_{ab} for a titanium spherical shell ($N_{11} = 0, M_{11} \neq 0$)

λ_0	a/h = 10		a/h = 5		a/h = 2		a/h = 1	
	$E_1/E_2 =$	$E_1/E_2 =$	$E_1/E_2 =$	$E_1/E_2 =$	$E_1/E_2 =$	$E_1/E_2 =$	$E_1/E_2 =$	$E_1/E_2 =$
	0.725	1.380	0.725	1.380	0.725	1.380	0.725	1.380
0.0	0.632	0.634	0.651	0.650	0.691	0.687	0.742	0.735
0.25	0.626	0.628	0.645	0.643	0.684	0.679	0.732	0.725
0.50	0.611	0.612	0.628	0.626	0.663	0.658	0.707	0.699
0.75	0.589	0.590	0.604	0.602	0.634	0.629	0.673	0.665
1.0	0.564	0.564	0.577	0.574	0.602	0.596	0.636	0.628
1.5	0.510	0.509	0.518	0.515	0.536	0.531		
2.0	0.458	0.457	0.463	0.460	0.479	0.473		
2.5	0.412	0.411	0.416	0.413				
3.0	0.373	0.372	0.377	0.374				
3.5	0.341	0.339	0.344	0.341				
4.0	0.314	0.312	0.318	0.313				

Table 11. The stress intensity factor ratio k_{ab} for a titanium spherical shell ($N_{11} = 0, M_{11} \neq 0$)

λ_0	a/h = 10		a/h = 5		a/h = 2		a/h = 1	
	$E_1/E_2 =$	$E_1/E_2 =$	$E_1/E_2 =$	$E_1/E_2 =$	$E_1/E_2 =$	$E_1/E_2 =$	$E_1/E_2 =$	$E_1/E_2 =$
	0.725	1.380	0.725	1.380	0.725	1.380	0.725	1.380
0.0	0.000	0.000	0.000	0.000	0.000	0.000	0.000	0.000
0.25	0.006	0.007	0.006	0.007	0.007	0.008	0.009	0.010
0.50	0.015	0.017	0.016	0.018	0.019	0.021	0.022	0.024
0.75	0.025	0.028	0.027	0.029	0.031	0.034	0.035	0.039
1.0	0.034	0.037	0.036	0.040	0.042	0.045	0.047	0.051
1.5	0.049	0.054	0.052	0.057	0.059	0.064		
2.0	0.061	0.066	0.064	0.069	0.071	0.076		
2.5	0.069	0.075	0.072	0.078				
3.0	0.074	0.081	0.078	0.084				
3.5	0.078	0.085	0.082	0.088				
4.0	0.081	0.088	0.084	0.091				

Table 12. The stress intensity factor ratio k_{mm} for a graphite spherical shell ($N_{11} \neq 0, M_{11} = 0$)

λ_0	a/h = 10		a/h = 5		a/h = 2		a/h = 1	
	$E_1/E_2 =$ 0.037	$E_1/E_2 =$ 26.667	$E_1/E_2 =$ 0.037	$E_1/E_2 =$ 26.667	$E_1/E_2 =$ 0.037	$E_1/E_2 =$ 26.667	$E_1/E_2 =$ 0.037	$E_1/E_2 =$ 26.667
0.0	1.000	1.000	1.000	1.000	1.000	1.000	1.000	1.000
0.25	1.006	1.073	1.006	1.073	1.006	1.074	1.006	1.075
0.50	1.024	1.250	1.024	1.251	1.024	1.255	1.026	1.267
0.75	1.051	1.491	1.052	1.493	1.053	1.504	1.059	1.540
1.0	1.089	1.767	1.090	1.771	1.095	1.794	1.108	1.863
1.5	1.190	2.377	1.193	2.387	1.207	2.445		
2.0	1.318	3.030	1.324	3.050	1.354	3.165		
2.5	1.470	3.713	1.480	3.748				
3.0	1.643	4.423	1.658	4.484				
3.5	1.835	5.164	1.857	5.271				
4.0	2.044	5.948	2.075	6.145				

Table 13. The stress intensity factor ratio k_{mm} for a graphite spherical shell ($N_{11} \neq 0, M_{11} = 0$)

λ_0	a/h = 10		a/h = 5		a/h = 2		a/h = 1	
	$E_1/E_2 =$ 0.037	$E_1/E_2 =$ 26.667	$E_1/E_2 =$ 0.037	$E_1/E_2 =$ 26.667	$E_1/E_2 =$ 0.037	$E_1/E_2 =$ 26.667	$E_1/E_2 =$ 0.037	$E_1/E_2 =$ 26.667
0.0	0.000	0.000	0.000	0.000	0.000	0.000	0.000	0.000
0.25	0.012	0.037	0.012	0.037	0.013	0.038	0.014	0.040
0.50	0.033	0.088	0.033	0.087	0.035	0.087	0.038	0.089
0.75	0.055	0.133	0.056	0.130	0.058	0.126	0.061	0.125
1.0	0.076	0.165	0.076	0.158	0.077	0.147	0.079	0.141
1.5	0.104	0.172	0.101	0.151	0.096	0.114		
2.0	0.111	0.084	0.103	0.041	0.091	-0.035		
2.5	0.099	-0.108	0.085	-0.179				
3.0	0.069	-0.404	0.048	-0.510				
3.5	0.022	-0.804	-0.006	-0.957				
4.0	-0.041	-1.314	-0.074	-1.538				

Table 14. The stress intensity factor ratio $k_{\theta\theta}$ for a graphite spherical shell ($N_{11} = 0, M_{11} \neq 0$)

λ_0	a/h = 10		a/h = 5		a/h = 2		a/h = 1	
	$E_1/E_2 =$ 0.037	$E_1/E_2 =$ 26.667	$E_1/E_2 =$ 0.037	$E_1/E_2 =$ 26.667	$E_1/E_2 =$ 0.037	$E_1/E_2 =$ 26.667	$E_1/E_2 =$ 0.037	$E_1/E_2 =$ 26.667
0.0	0.615	0.599	0.635	0.611	0.686	0.639	0.751	0.677
0.25	0.611	0.593	0.631	0.604	0.680	0.631	0.744	0.666
0.50	0.600	0.577	0.618	0.587	0.664	0.611	0.723	0.642
0.75	0.584	0.556	0.600	0.564	0.640	0.585	0.695	0.612
1.0	0.564	0.533	0.578	0.539	0.613	0.556	0.664	0.580
1.5	0.518	0.486	0.527	0.490	0.555	0.501		
2.0	0.472	0.442	0.478	0.443	0.504	0.451		
2.5	0.430	0.402	0.435	0.402				
3.0	0.394	0.367	0.399	0.367				
3.5	0.364	0.336	0.369	0.335				
4.0	0.339	0.309	0.346	0.308				

Table 15. The stress intensity factor ratio $k_{\theta\theta}$ for a graphite spherical shell ($N_{11} = 0, M_{11} \neq 0$)

λ_0	a/h = 10		a/h = 5		a/h = 2		a/h = 1	
	$E_1/E_2 =$ 0.037	$E_1/E_2 =$ 26.667	$E_1/E_2 =$ 0.037	$E_1/E_2 =$ 26.667	$E_1/E_2 =$ 0.037	$E_1/E_2 =$ 26.667	$E_1/E_2 =$ 0.037	$E_1/E_2 =$ 26.667
0.0	0.000	0.000	0.000	0.000	0.000	0.000	0.000	0.000
0.25	0.003	0.008	0.003	0.008	0.004	0.010	0.004	0.011
0.50	0.007	0.019	0.008	0.021	0.010	0.024	0.012	0.027
0.75	0.013	0.032	0.014	0.034	0.017	0.038	0.020	0.043
1.0	0.018	0.043	0.019	0.046	0.023	0.051	0.027	0.057
1.5	0.027	0.063	0.029	0.066	0.033	0.072		
2.0	0.033	0.077	0.035	0.080	0.040	0.087		
2.5	0.038	0.087	0.040	0.090				
3.0	0.041	0.094	0.043	0.098				
3.5	0.043	0.099	0.045	0.103				
4.0	0.044	0.103	0.046	0.108				

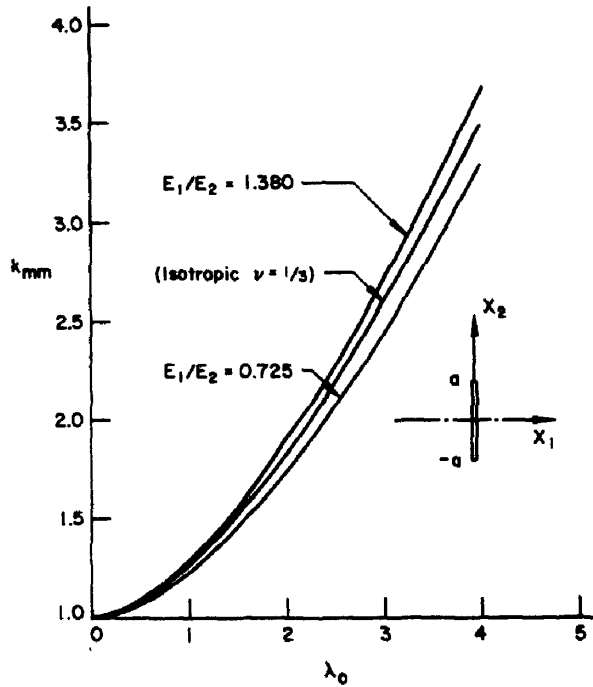


Fig. 3. The membrane component of the stress intensity factor ratio k_{mm} in an isotropic and in a specially orthotropic spherical (titanium) shell; $a/h = 5$, $\lambda_0^4 = 12(1-\nu^2)a^4/R^2h^2$, $\nu = 1/3$ for isotropic shell, $\nu = \sqrt{\nu_1\nu_2}$ for orthotropic shell.

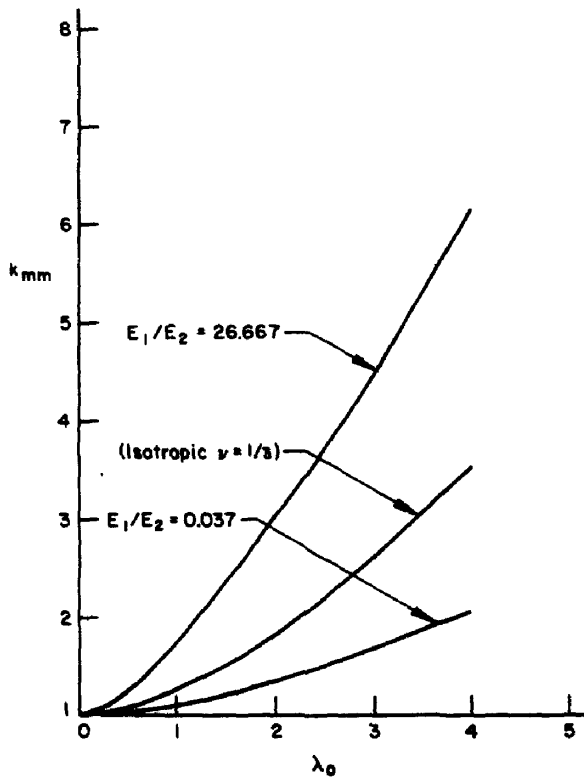


Fig. 4. The membrane component of the stress intensity factor ratio k_{mm} in an isotropic and in a specially orthotropic spherical (graphite) shell; $a/h = 5$, $\lambda_0^4 = 12(1-\nu^2)a^4/R^2h^2$, $\nu = 1/3$ for isotropic shell, $\nu = \sqrt{\nu_1\nu_2}$ for orthotropic shell.

Acknowledgements—This study was supported by NASA-Langley under the Grant NGR39-007-011, the National Science Foundation under the Grant ENG77-19127, and the U.S. Department of Transportation under the Contract DOT-RC-82007.

REFERENCES

1. L. G. Copley and J. L. Sanders, Jr., A longitudinal crack in a cylindrical shell under internal pressure. *Int. J. Fract. Mech.* **5**, 117–131 (1969).
2. E. S. Folias, An axial crack in a pressurized cylindrical shell. *Int. J. Fract. Mech.* **1**, 104–113 (1965).
3. F. Erdogan and J. J. Kibler, Cylindrical and spherical shells with cracks. *Int. J. Fract. Mech.* **5**, 229–237 (1969).
4. F. Erdogan and M. Ratwani, Fatigue and fracture of cylindrical shells containing a circumferential crack. *Int. J. Fract. Mech.* **6**, 379–392 (1970).
5. J. G. Simmonds, M. R. Bradley and J. W. Nicholson, Stress intensity factors for arbitrarily oriented cracks in shallow shells. *J. Appl. Mech.* **45**, *Trans. ASME* 135–141 (1978).
6. F. Erdogan, Crack problems in cylindrical and spherical shells. *Plates and Shells with Cracks* (Edited by G. C. Sih), pp. 161–199. Noordhoff, Leyden (1977).
7. M. L. Williams, The bending stress distribution at the base of a stationary crack. *J. Appl. Mech.* **28**, *Trans. ASME* 78–82 (1961).
8. J. K. Knowles and N. M. Wang, On the bending of an elastic plate containing a crack. *J. Math. Phys.* **39**, 223–236 (1960).
9. N. M. Wang, Effects of plate thickness on the bending of an elastic plate containing a crack. *J. Math. Phys.* **47**, 371–390 (1968).
10. R. J. Hartranft and G. C. Sih, Effect of plate thickness on the bending stress distribution around through cracks. *J. Math. Phys.* **47**, 276–291 (1968).
11. E. Reissner, On bending of elastic plates. *Quart. Appl. Math.* **5**, 55–68 (1947).
12. P. M. Nagdi, Note on the equations of shallow elastic shells. *Quart. Appl. Math.* **14**, 331 (1956).
13. S. Krenk, Influence of transverse shear on an axial crack in a cylindrical shell. *Int. J. Fract.* **14**, 123–143 (1978).
14. F. Delale and F. Erdogan, Transverse shear effect in a circumferentially cracked cylindrical shell. *Quart. Appl. Math.* **37** (1979).
15. G. C. Sih and H. C. Hagedorn, A new theory of spherical shells with cracks. In *Thin-Shell Structures: Theory, Experiment and Design* (Edited by Y. C. Fung and E. E. Sechler). Prentice Hall, Englewood Cliffs, New Jersey (1974).
16. N. I. Muskhelishvili, *Singular Integral Equations*. Noordhoff, Groningen (1953).
17. I. S. Gradshteyn and I. M. Ryzhik, *Tables of Integrals, Series and Products*. Academic Press, New York (1965).
18. F. Erdogan, Mixed boundary-value problems in mechanics. *Mechanics Today* (Edited by S. Nemat-Nasser), Vol. 4, p. 1. Pergamon Press, Oxford (1978).
19. P. S. Theocaris and N. I. Ioakimidis, Numerical integration methods for the solution of singular integral equations. *Quart. Appl. Math.* **35**, 173–183 (1977).
20. S. Krenk, Quadrature formulae of closed type for solution of singular integral equations. *J. Inst. Maths. Appl.* **22**, 99–107 (1978).

APPENDIX A

The dimensionless quantities

$$x = \frac{1}{\sqrt{c}} \frac{X_1}{a}, \quad y = \sqrt{c} \frac{X_2}{a}, \quad z = \frac{X_3}{a}, \quad (\text{A.1})$$

$$u = \sqrt{c} \frac{U_1}{a}, \quad v = \frac{1}{\sqrt{c}} \frac{U_2}{a}, \quad w = \frac{W}{a}, \quad (\text{A.2})$$

$$\beta_r = \sqrt{c} \beta_1, \quad \beta_\theta = \frac{1}{\sqrt{c}} \beta_2, \quad \phi = \frac{F}{a^2 h E}$$

$$\sigma_{rr} = \frac{\sigma_{11}}{c E}, \quad \sigma_{\theta\theta} = \frac{c \sigma_{22}}{E}, \quad \sigma_{rz} = \frac{\sigma_{12}}{E} \quad (\text{A.3})$$

$$N_{rr} = \frac{N_{11}}{c h E}, \quad N_{\theta\theta} = \frac{c N_{22}}{h E}, \quad N_{rz} = \frac{N_{12}}{h E} \quad (\text{A.4})$$

$$M_{rr} = \frac{M_{11}}{c h^2 E}, \quad M_{\theta\theta} = \frac{c M_{22}}{h^2 E}, \quad M_{rz} = \frac{M_{12}}{h^2 E} \quad (\text{A.5})$$

$$V_r = \frac{V_1}{\sqrt{c h B}}, \quad V_\theta = \frac{\sqrt{c} V_2}{h B}, \quad (\text{A.6})$$

$$\lambda_1^4 = 12(1 - \nu^2) \frac{c^2 a^4}{h^2 R_1^2}, \quad \lambda_2^4 = 12(1 - \nu^2) \frac{a^4}{c^2 h^2 R_2^2},$$

$$\lambda_{12}^4 = 12(1 - \nu^2) \frac{a^4}{h^2 R_{12}^2}, \quad \lambda^4 = 12(1 - \nu^2) \frac{a^2}{h^2}, \quad \kappa = \frac{E}{B \lambda^3}. \quad (\text{A.7})$$